


DATA NOTE

Long-read only assembly of *Drechmeria coniospora* genomes reveals widespread chromosome plasticity and illustrates the limitations of current nanopore methods

Damien Courtine ¹, Jan Provaznik ², Jerome Reboul ^{1,3},
Guillaume Blanc ⁴, Vladimir Benes ² and Jonathan J. Ewbank ^{1,*}

¹Aix-Marseille University, CNRS, INSERM, CIML, Turing Centre for Living Systems, Marseille, France;

²European Molecular Biology Laboratory (EMBL), GeneCore, Heidelberg, Germany; ³Present address: Institut de Génétique Moléculaire de Montpellier, Montpellier, France and ⁴Aix-Marseille University, Université de Toulon, CNRS, IRD, MIO UM 110, 13288 Marseille, France

*Correspondence address. Jonathan Ewbank, CIML, Case 906, 13288 Marseille cedex 9, France. Tel/Fax: +33-4-91-26-94-72; E-mail: ewbank@ciml.univ-mrs.fr  <http://orcid.org/0000-0002-1257-6862>

Abstract

Background: Long-read sequencing is increasingly being used to determine eukaryotic genomes. We used nanopore technology to generate chromosome-level assemblies for 3 different strains of *Drechmeria coniospora*, a nematophagous fungus used extensively in the study of innate immunity in *Caenorhabditis elegans*. **Results:** One natural geographical isolate demonstrated high stability over decades, whereas a second isolate not only had a profoundly altered genome structure but exhibited extensive instability. We conducted an in-depth analysis of sequence errors within the 3 genomes and established that even with state-of-the-art tools, nanopore methods alone are insufficient to generate eukaryotic genome sequences of sufficient accuracy to merit inclusion in public databases. **Conclusions:** Although nanopore long-read sequencing is not accurate enough to produce publishable eukaryotic genomes, in our case, it has revealed new information about genome plasticity in *D. coniospora* and provided a backbone that will permit future detailed study to characterize gene evolution in this important model fungal pathogen.

Keywords: DNA sequencing; Oxford Nanopore Technologies; endoparasite; fungus; nematode; base-calling; assembly algorithms; homopolymer

Background

Drechmeria coniospora (NCBI:txid98403) is an obligate parasitic fungus belonging to the order of Hypocreales. This fungus forms spores that adhere to the cuticle of a range of different nematodes to infect them [1]. We adopted *D. coniospora* strain ATCC 96-282, derived from a strain isolated in Sweden, as a model

pathogen for *Caenorhabditis elegans* 20 years ago [2]. We have cultured this strain, referred to here as Swe1, continuously since then, using it to understand innate immune mechanisms in its nematode host [3, 4].

As part of our characterization of the interaction between *D. coniospora* and *C. elegans*, in 2013, we extracted DNA from our laboratory strain of the time (referred to here as Swe2) and deter-

Received: 17 December 2019; Revised: 17 April 2020; Accepted: 2 September 2020

© The Author(s) 2020. Published by Oxford University Press GigaScience. This is an Open Access article distributed under the terms of the Creative Commons Attribution License (<http://creativecommons.org/licenses/by/4.0/>), which permits unrestricted reuse, distribution, and reproduction in any medium, provided the original work is properly cited.

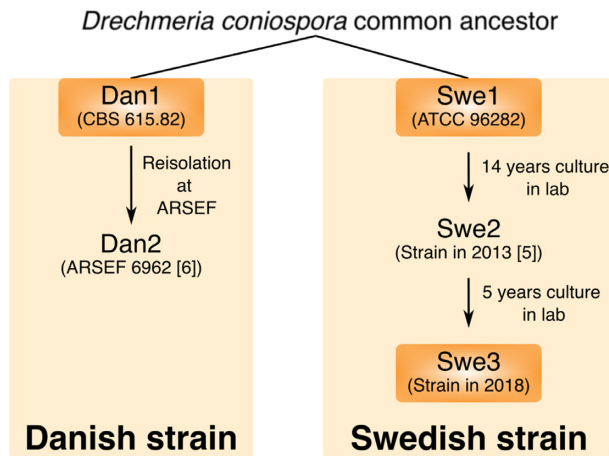


Figure 1: An overview of *D. coniospora* strain isolation and culture history. A strain of *D. coniospora* collected from Denmark in 1982 at the latest was deposited at the CBS-KNAW culture collection, now held by the Westerdijk Fungal Biodiversity Institute as CBS615.82. It was transferred in 1987 to the ARS Collection of Entomopathogenic Fungal Cultures (as ARSEF 2468) and then re-isolated in 2001 as ARSEF 6962. A second strain collected from Sweden was deposited at the American Type Culture Collection as ATCC 96-282. It has been cultured through serial passage in *C. elegans* continuously since 1999.

mined its genome. Despite attempts to complete the assembly, the Swe2 genome remained fragmented, with an N50 of 3.86 Mb [5]. In addition to the genome of Swe2, a second *D. coniospora* genome is available (referred to here as Dan2) [6], derived from a strain related to a Danish isolate (Dan1; Fig. 1). Although corresponding to a chromosome-level assembly, this latter genome still contains large stretches (up to 500 kb) of undetermined sequence. In this study, we used Oxford Nanopore Technology (ONT) long-read sequencing to assemble complete fungal genomes. This revealed that the 2 isolates (Swe1 and Dan1) display strikingly different levels of genomic stability. We provide a detailed analysis that illustrates the continuing challenges to using only ONT long-read sequencing for genome assembly. Because the genome sequences were of insufficient quality to allow accurate gene prediction, we polished the genomes using short DNA reads to generate high-quality sequences, providing a resource for future comparative studies.

Results

An all-against-all *in silico* genome comparison of the 2 publicly available *D. coniospora* genome sequences, for Dan2 [6] and Swe2 [5], indicated the presence of extensive genomic rearrangements (Fig. 2A). These could reflect real differences or assembly errors in 1 or both genomes. We directly confirmed 1 major rearrangement by PCR (Fig. 2B and C), suggesting that the differences could be real. To characterize this genomic plasticity, we determined the genomes of 3 strains related to the 2 that had been sequenced previously (Fig. 1). We used ONT nanopore sequencing to generate long reads and current assembly tools to construct chromosome-level assemblies for all 3 strains (Supplementary Fig. S1, Supplementary Table S1). Manual curation allowed complete ~30 kb mitochondrial genomes to be predicted from the assemblies generated by Canu [7].

All 3 nuclear genomes were divided in 3 similarly sized chromosomes, an unusual arrangement for such a fungus, as previously noted by Zhang et al. for Dan2 [6]. For the 2 strains related to Swe2, there was almost complete synteny of their nuclear

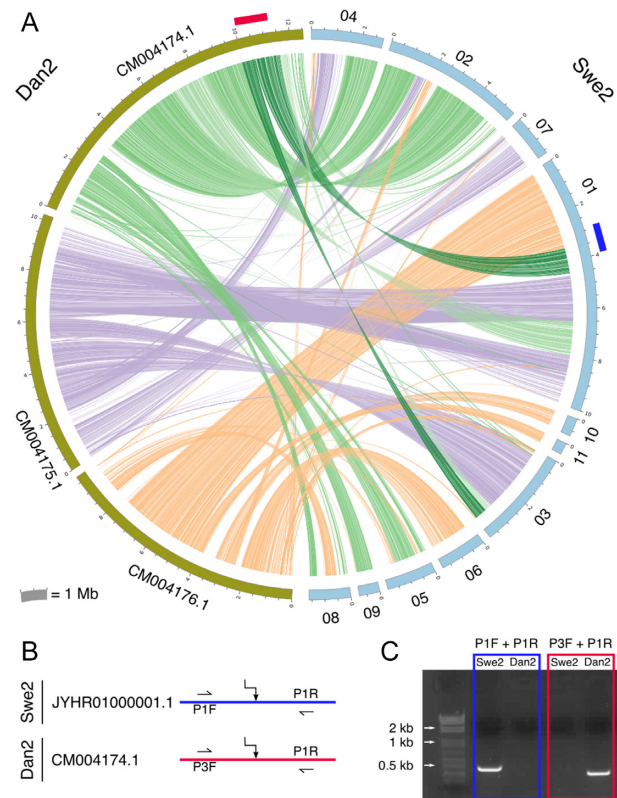


Figure 2: Inter-chromosomal rearrangements between strains Swe2 and Dan2. A. Circos plot representing regions >6 kb that are very similar between Dan2 (left, olive) and Swe2 (right, light blue) assemblies as determined by an all-against-all LAST analysis. Swe2 contig numbers are the last 2 digits of the accession ID (shown in B), preceding the suffix. Red and dark blue rectangles represent rearrangement junctions probed by PCR. B. Conceptual design of the PCR primers. C. Amplicons from the PCR were visualized after electrophoresis. Each pair gave 1 specific band of the expected size. The colour code is the same for the 3 panels.

genomes. Inspection of the 1 anomalous region in Swe1 where synteny broke down revealed that it was supported by only 1 long (215 kb) read and corresponded to a local discontinuity in the read coverage, as well as a break in the alignment between Canu-generated contigs and unitigs. All these factors indicated that this was an assembly artefact with a contig misassembled on the basis of an individual very long chimeric read (Supplementary Fig. S2). The same was true for the distinct unique non-syntentic region of the Swe3 assembly (Supplementary Fig. S3).

These were exceptional cases because almost all chimeric reads were identified and either trimmed or excluded from the assembly process by Canu (Supplementary Figs S4 and S5). An in-depth analysis of the Swe1 chimeric reads revealed that a large proportion were in fact the consequence of sequencing errors. In almost 40% of cases (1,010 of 2,566), the 2 regions flanking the presumptive site of chimerism mapped to within 50 nucleotides of each other on the corresponding single scaffold. There was no discernible pattern to the distribution of this interval in the remaining candidate chimeric reads (Supplementary Fig. S6A and B), nor were there any regions that were more likely to be the site of chimeric junctions (Supplementary Fig. S6C).

Notably the single chimeric read that escaped censoring, leading to a misassembly of Swe1, was not identified by the dedicated tool YACRD but was flagged as anomalous in reads recalled by Guppy (see Methods). This is an indication of the continuing improvement to base-calling tools. Also, these specific Swe1 and

Swe3 misassemblies were absent from the corresponding chromosome assemblies produced by the *de novo* assembler Flye [8] (Fig. 3A). This latter, however, introduced other assembly artefacts, including an erroneous fusion of contigs for the Dan1 assembly. This could not be ascribed to the inclusion of chimeric reads but rather seemed to result from the incorrect treatment of repeat sequences, including telomeric repeats at the extremity of 1 of the fused contigs (Fig. 3B–D). These results illustrate the interest of using >1 tool to aid in genome assembly. Therefore, starting with the Canu-generated sequences, we manually corrected anomalous regions and thereby produced assemblies for Swe1 and Swe3 that were entirely collinear (Fig. 4A).

These 2 genomes have 3 large chromosomes (8.5, 11.6, and 11.6 Mb), each with identifiable telomeric [9] and centromeric regions, indicating that the overall genome structure has remained constant over 20 years of laboratory culture. This allowed us then to use the Swe1 sequence to scaffold the fragmented Swe2 genome (Fig. 4B). To our great satisfaction, we were able to produce an entirely collinear chromosome-scale assembly. Thus, it appears that there were no assembly errors in the published Swe2 genome; it was simply incompletely scaffolded. This applies equally to the genomic regions containing copies of some mitochondrial genes that we previously suggested might indicate assembly errors [5]. They were revealed to be accurate; *D. coniospora* has nuclear paralogous copies of 10 mitochondrial protein-coding and 15 transfer RNA genes (so-called “numts” [nuclear sequences of mitochondrial origin] [10]). These results give further support to the existence of long-term stability of the genome of the Swe2-related strains. A whole-genome comparison between Swe1 and Dan2, however, revealed multiple and extensive genome rearrangements, involving intra- and inter-chromosomal translocations and inversions (Fig. 4C).

Using the same strategy described above, we assembled and polished the Dan1 genome to give chromosome-level sequences. When we compared Dan1 and Dan2, we were surprised to find 2 major events of reciprocal exchange of chromosome ends, and an intra-chromosomal inversion (Fig. 4D). These events were supported in a coherent and consistent manner by all the available data (Supplementary Fig. S7). In other fungal species, such chromosomal rearrangements have been reported to be the result of ectopic recombination between non-allelic homologous sequences, including repeated DNA elements [11, 12]. A search of the 50kb regions flanking each break point for transposable elements [13] and repetitive DNA families [14] failed to reveal any significant repeat sequence signature (see Supplementary Methods). Because the Dan2 assembly is of high confidence, supported by long reads and optical mapping [6], given the short time of *in vitro* culture that separates it from Dan1, this suggests that the genome of the Dan1 isolate is not stable.

In alignments of the sequence of Swe1, generated using only nanopore reads, with that of Swe2, there were stretches of complete nucleotide identity extending over >25 kb. This is a testament to the general reliability of nanopore sequencing. We therefore identified the complete set of proteins identical in Swe2 and Dan2 corresponding to single-copy, single-exon genes (see Methods). These would be expected to be present in the newly assembled Swe1, Swe3, and Dan1 genomes. Indeed, using these 305 genes as a query, we could identify homologous sequences for each in all 3 genomes. Fewer than one-sixth of the corresponding genes, however, were predicted to encode full-length proteins in any of the 3 new genomes (Fig. 5A). While nanopore reads are very useful for genome assembly, they are hindered by a high error rate, especially in homopolymer stretches. Sequence quality can be improved using polishing

tools that aim to ameliorate consensus sequences generally by going back to raw reads and applying integrative algorithms [15]. In our case, applying current best practices, while providing a very substantial improvement (up to 5-fold in the best case), did not take the prediction level beyond 82% accuracy. The quality of the prediction seen with the Dan1 genome was strikingly lower than that of the other 2 genomes (Fig. 5A, Supplementary Table S1).

Inspection suggested that the majority of errors were in homopolymer sequences, as expected, with nucleotide insertions and deletions leading to alterations of the reading frame. To investigate this poor homopolymer predictive performance systematically, we computed the number of G/C or A/T homopolymer stretches of ≥ 4 nucleotides for each of the 305 genes. We plotted these values, indicating the proportion of genes that encoded the expected full-length predicted protein for each of the 3 genomes. While there was the expected inverse relationship between accuracy and the number of homopolymer stretches, there were striking exceptions. Curiously some of these exceptions were specific to a single genome (Fig. 5B–D). Furthermore, and unexpectedly, polishing introduced more nucleotide insertion errors than deletions, frequently on the basis of tenuous read support. Overall, however, there was no obvious pattern to explain why errors were introduced, given the underlying reads used to build the consensus sequence (Supplementary Table S2).

During the inspection of the assembled and polished genomes, we found 2 other types of anomalies. The first concerned the regions flanking the nuclear genomic copies of mitochondrial genes (numts), where polishing added short extraneous low-complexity sequences (mean length 15 nt, mainly As or Ts), for which, surprisingly, there was no sequence support from the reads used by the assembler (Fig. 6A). This probably arose because of the very high nucleotide similarity between regions of the nuclear and mitochondrial genomes that extended across >25 kb, including a repeat of 9.8 kb (Supplementary Fig. S8A and B). Notably, despite using high-coverage ONT long reads, we could not establish with absolute certainty the precise copy number for the unit sequence in the Swe genomes (Supplementary Fig. S8B).

In the second case, for the Swe3 genome, a large (~10 kb) region, with a complex sequence, well supported by the Canu-corrected and trimmed reads, was inexplicably excluded from the initial Canu assembly and only imprecisely restored by polishing (Fig. 6B and C, Supplementary Fig. S8C). Here, while there was no evidence for repeated DNA elements on both sides of the point of sequence discontinuity, there was a single such 1.2 kb duplication (Supplementary Fig. S8C and D). These few regions were identified because of discontinuities in the depth of read coverage, which otherwise was remarkably constant across the complete genomes. With the resolution of these assembly errors, we were able to generate complete genomes of high overall structural quality using ONT long reads only.

As explained above, however, these assemblies were not of sufficient sequence quality to allow accurate gene prediction. Therefore, to extend our analysis, we used Illumina sequencing to generate very deep short-read coverage for the Swe1, Swe3, and Dan1 genomes. This allowed high-quality final sequences to be generated for all 3 strains. While short-read-based polishing did not alter the global structure, it allowed homopolymer length errors to be corrected and the generation of entirely contiguous chromosome sequences (Supplementary Table S1).

To confirm the correctness of the short-read polished assemblies, we returned to our 305 single-copy orthologues. After the short-read polishing, all 305 genes could be identified in each of

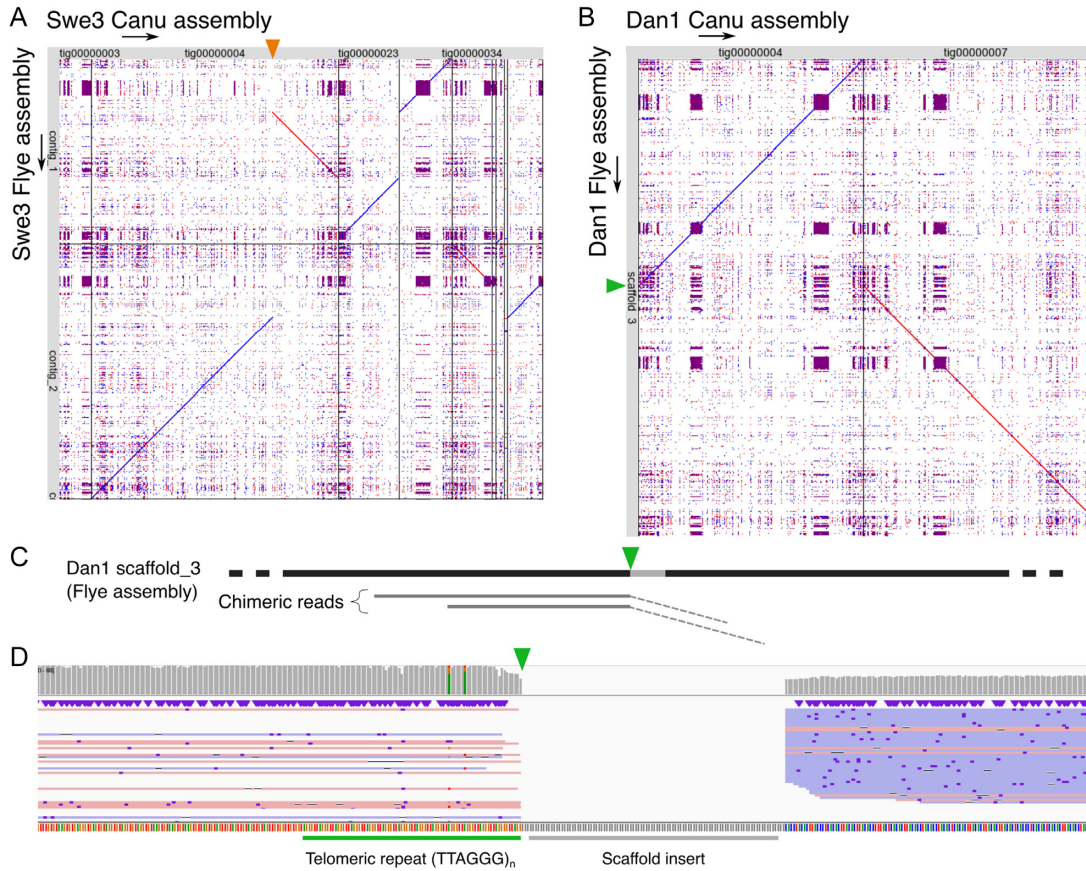


Figure 3: Comparisons between Canu and Flye assemblies. A, B. Dot-plots of the non-congruent assemblies generated by Canu (x-axis) against those generated by Flye (y-axis) for the Swe3 (A) and Dan1 (B) genomes. The orange triangle (A) marks the position where the Canu contig tig00000004 was split during the manual curation because of its chimeric nature. The green triangle (B) marks the position of a Flye scaffolding error. C. Schematic representation of the Dan1 Flye assembly, showing the mapping of chimeric reads close to the scaffolding error (green triangle). The coordinates in parentheses are the mapping positions of the clipped part of the reads (dashed line) on another contig of the assembly. Notably, this error was eliminated when these chimeric reads were excluded from the input data. D. Mapping of long reads close to the scaffolding error (green triangle) on the Dan1 Flye assembly. The green bar marks the telomeric tandem repeat motif. The grey bar indicates the 100 Ns inserted by Flye to unite the scaffold.

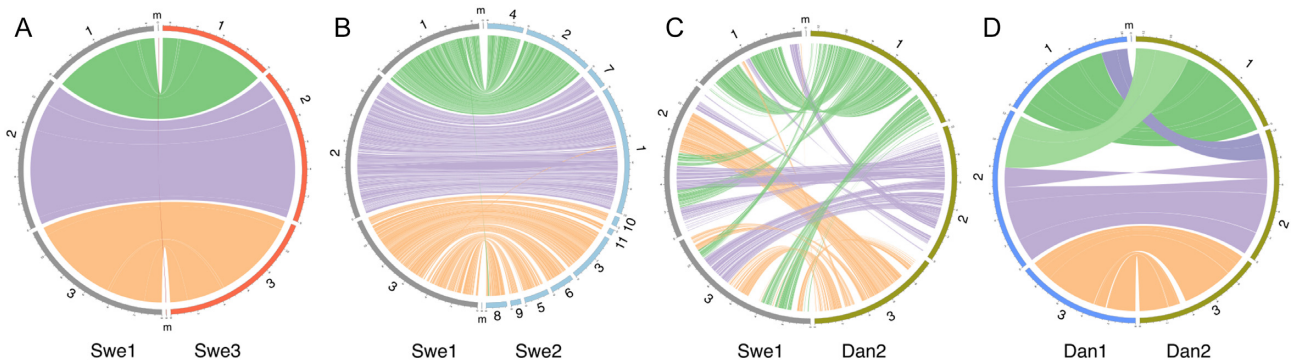


Figure 4: Synteny among the genomes of 5 *D. coniospora* strains. Circos plot representing regions >20 kb that are very similar between assemblies as determined by all-against-all LAST analyses. Each assembly is shown at the same scale and in the same order and orientation across panels.

the 3 genomes (Supplementary Table S1). We also benchmarked our successive assemblies using BUSCO that searches for a set of universal single-copy orthologues (USCOs) by sequence similarity. While the initial genome assemblies gave low scores, with ~65% of complete USCOs and 35% fragmented or missing (Table 1), after long-read polishing the score for complete USCOs increased up to as high as 97%. Given the demonstrably low

quality of the genome sequences (Fig. 5), we investigated the basis of this disparity. We identified among the USCOs those that corresponded to single-exon genes in the Dan2 and Swe2 reference genomes. These genes were then used as queries for high-stringency searches of the Dan1, Swe1, and Swe3 genomes at successive steps of assembly and polishing and the results compared with the results of the corresponding BUSCO analysis.

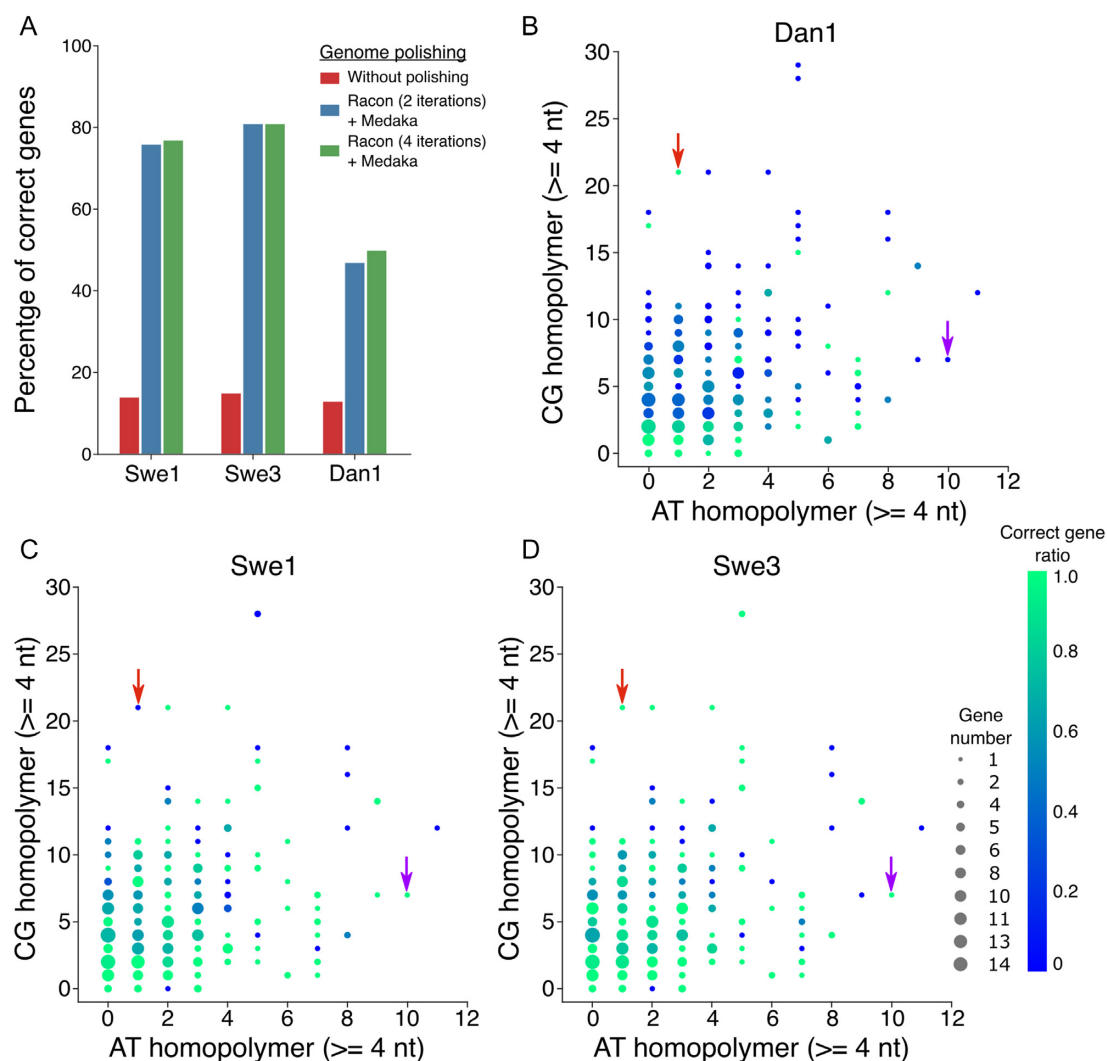


Figure 5: Evaluation of sequence errors in the 3 new genomes. A. Percentage of correct genes (based on length of the corresponding predicted protein) among 305 conserved genes, for the 3 new genomes, in the initial assembly and after 2 different polishing strategies. B, C, D. Scatter plots of homopolymer composition (A/T or C/G) and accuracy among the same 305 conserved genes for Dan1 (B), Swe1 (C), and Swe3 (D). The dot size is proportional to the number of genes, and the colour indicates the proportion of genes predicted to be correct. Red and purple arrows highlight 2 particular cases, among many, where homopolymer errors are only present in 1 genome.

Table 1: BUSCO results. Percentage of each category of the expected 1,315 USCOs for different genome assemblies. Of the 11 USCOs missing in Swe1 and Swe3, 10 are also absent from Swe2, and 9 from Dan1 (and Dan2). These are therefore likely to be real gene losses in *D. coniospora*, so that only 2 USCOs (0.2%) at most are missing.

Strain	Assembly	All	Complete, No. (%)			Missing
			Single	Duplicated	Fragmented	
Dan1	Canu curated	820 (62.4)	820 (62.4)	0	259 (19.7)	236 (17.9)
	Long-read polish	1,187 (90.3)	1,187 (90.3)	0	62 (4.7)	66 (5)
	Short-read polish	1,297 (98.6)	1,296 (98.6)	1 (0.1)	9 (0.7)	9 (0.7)
Dan2	[6]	1,298 (98.7)	1,297 (98.6)	1 (0.1)	8 (0.6)	9 (0.7)
Swe1	Canu curated	869 (66.1)	868 (66)	1 (0.1)	243 (18.5)	203 (15.4)
	Long-read polish	1,266 (96.6)	1,266 (96.6)	0	21 (1.6)	28 (2.1)
	Short-read polish	1,296 (98.6)	1,295 (98.5)	1 (0.1)	8 (0.6)	11 (0.8)
Swe2	[5]	1,296 (98.6)	1,294 (98.4)	2 (0.2)	9 (0.7)	10 (0.8)
Swe3	Canu curated	859 (65.3)	858 (65.2)	1 (0.1)	243 (18.5)	213 (16.2)
	Long-read polish	1,274 (96.9)	1,274 (96.9)	0	17 (1.3)	24 (1.8)
	Short-read polish	1,295 (98.5)	1,294 (98.4)	1 (0.1)	9 (0.7)	11 (0.8)

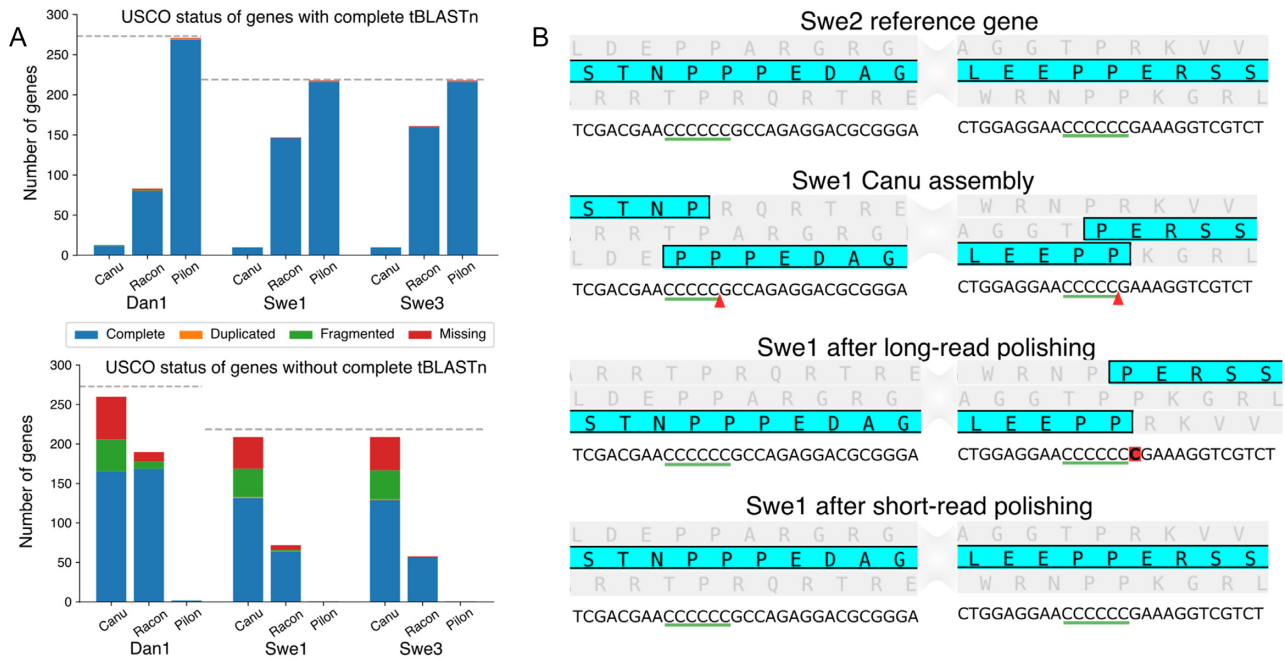


Figure 7: Example of sequence errors introduced during assembly and polishing. Stacked bar plot of USCO status for the orthologues of selected mono-exonic Swe2 or Dan2 genes classified according to the result of a TBLASTN search against the indicated assembly (Canu: from Canu; Racon: after long-read polish; Pilon: after short-read polishing). B. Detailed view of 2 parts of RJ55.06485 from the Swe2 reference genome each containing a homopolymer sequence (green underscore) and the corresponding positions in successive Swe1 assemblies. For each, the predicted protein sequence, highlighted in turquoise, with the other open reading frames in grey, is shown above the corresponding nucleotide sequence. The red arrowheads highlight the missing nucleotides; the extraneous nucleotide is boxed in red.

to those for the previous Dan2 and Swe2 assemblies. The new Swe1, Swe3, and Dan1 genomes therefore represent the starting point for future detailed analysis to characterize the molecular evolution of *D. coniospora*.

Discussion

Previous genome assemblies for *D. coniospora* required a combination of sequencing approaches [5, 6]. Here, using only long reads and Canu, we produced the first complete circular mitochondrial genome for *D. coniospora* and were able to generate chromosome-scale assemblies for the nuclear genome. The rare misassembled contigs, formed by Canu because of single very long chimeric reads, as previously described [16], could be detected by read coverage anomalies and comparisons with unitigs, suggesting that solutions to avoid their creation could be implemented within Canu. The majority of reads that were flagged as chimeric arose from sequencing or polishing errors. They reflected a short (<50 bp) discrepancy between the individual reads and the final sequence. There was no indication of any sequence bias at the break points of the remaining chimeric reads, supporting the notion that these reads arise from excessively rapid reloading of the sequencing pore [17].

The use of other genome assembly tools, and the comparison of assembly discrepancies, is an additional method to produce high-confidence genomes. Here, we used Flye, which for these genomes required run times that were 10-fold shorter than Canu. A comparison of the assemblies highlighted ambiguous regions in the genome that could then be resolved by manual inspection. On the other hand, Flye was confounded by telomeric repeats. Because telomeres can be identified on the basis of their sequence, there is also clear room for algorithmic

improvement to Flye through the explicit definition of chromosome ends.

One clear and well-established advantage of using long reads is the possibility of resolving very extended stretches of complex tandem repeats (VeCTRs) [18] and other repetitive sequences including centromeres. These correspond to most of the breaks in the continuity of the published Swe2 genome. In addition to acrocentric regional centromeres, Zhang et al. reported the presence of a vestigial centromere from a putative chromosomal fusion event [6]. These were also found in the fully assembled Swe1 and Swe3 genomes, indicating that chromosomal fusions were present in the common ancestor of the Swe1 and Dan1 strains.

For Swe1, Swe3, and Dan1 we were able to reconstruct complete mitochondrial genomes, with features typical of fungi of the order Hypocreales. On the other hand, unlike Dan1 (and Dan2), the nuclear genomes of Swe1 and its derivatives Swe2 and Swe3 contained different numbers of copies of sequence very similar to parts of their own mitochondrial DNA. This type of event, and more generally repeated regions with long and nearly identical sequences, are more readily detectable with long reads [19] and are particularly challenging for polishing even with short reads [20].

The duplication of mitochondrial genes in the nuclear genome has been described in other fungal genomes [10] and must have occurred after the divergence of Dan1 and Swe1. Despite this genome plasticity, even after 20 years of continuous laboratory culture the Swe1 and Swe3 genomes were entirely collinear. This contrasts with the rearrangements seen between the Dan1 and Dan2 genomes, which in principle should be from strains that have had little opportunity to diverge (L. Castrillo, Curator, ARS Collection of Entomopathogenic Fungal Cultures, personal communication). It will be interesting in the future to

characterize the reasons for the marked difference in genomic stability between Dan1 and Swe1.

The accuracy of ONT long-read sequencing is increasing because of improvements in the chemistry used and signal detection, as well as base-calling [21]. Despite good read depth, however, our assemblies were not of sufficient quality at the nucleotide level to allow accurate gene prediction. Furthermore, we noted that although polishing using only long reads dramatically increased overall sequence accuracy, it introduced errors around the numts. Similar errors during polishing of near-identical sequences have been noted in ONT-based metagenomic studies [22]. Despite these limitations, research groups are publishing and submitting to public sequence databases genomes for fungi, plants, and animals based on nanopore sequencing alone (86 for eukaryotes in addition to the 134 bacterial genomes in “Assembly” from GenBank release 236 from 15 February 2020). This is problematic because low-quality genome sequences compromise the accuracy of sequence similarity searches in public databases. On the basis of our results, a re-analysis of the completeness of these “nanopore-only” genomes is merited, to confirm that they are indeed of low quality. Similar concerns do not apply to fungal genomes assembled using only long reads generated with Pacific Biosciences technology [23] because these are not hindered by the intrinsic problem of homopolymer length errors that we found to be the most significant quality barrier when using ONT reads. On the basis of our detailed analysis and in line with the consensus regarding *de novo* assembly with ONT long reads (e.g., [24]), we polished our 3 assemblies with short reads. This greatly improved their quality.

Regarding the homopolymer sequence errors, as noted above, they were not consistent across the sequenced genomes; even between Swe1 and Swe3 there were instances of widely differing rates of errors in orthologous genes, despite very similar underlying reads. Indeed there was no clear pattern in the inaccuracies, which will render bioinformatic approaches to remedy this problem more difficult. On the other hand, the errors were more often overprediction of homopolymer length, despite having a majority of reads supporting the correct sequence. It is possible that polishing tools have not kept pace with improvements in base-calling, leading to an overcompensation in the inference of homopolymer length.

It is standard practice to check the completeness of *de novo* genome assemblies with a strategy based on the detection of predicted groups of conserved orthologous proteins. One popular and much-cited tool is BUSCO [25], which was developed before ONT-based sequencing became prevalent. Because BUSCO relies on *in silico* translation, small indels can be overlooked because the resulting virtual sequence can be recapitulated despite a frameshift. This explains the disparity between the BUSCO results and our own analyses that were deliberately restricted to mono-exonic genes. Contrary to BUSCO, our analysis indicated that roughly one-fifth of the genes after long-read polishing had an incorrect sequence. Current BUSCO-type approaches, based on sequence similarity and not excluding genes with improbably short introns, cannot be used as a quality metric for ONT-only assemblies and are appropriate only after short-read correction.

Conclusions

Nanopore long-read sequencing provides a powerful way to assemble complex genomes with limited manual curation but still falls short of the quality required to produce publishable eukary-

otic genomes. In our case, it has revealed new information about genome plasticity in *D. coniospora* and provided a backbone that will permit future detailed study to characterize gene evolution in this important model fungal pathogen.

Methods

DNA extraction

D. coniospora spores were cultured in liquid NGMY medium [26] at 37°C for 5 days. Fungal DNA was extracted according to a published protocol (from p. 13 onwards of [27]) [28], with the following modifications: instead of centrifugation to collect DNA after precipitation with isopropanol, we recovered the DNA filaments with a glass hook, washed and dried them as described [29], and resuspended the DNA without agitation in Tris-EDTA buffer.

Nanopore sequencing library preparation

Libraries were prepared for sequencing on GridION (GridION Mk1, [RRID:SCR.017986](#)) with the ligation sequencing kit SQK-LSK109. The GridION sequencing was run on flowcell FLO-MIN106 for 47, 48, and 48 hours using 972, 660, and 610 ng of DNA (for Swe3, Swe1, and Dan1, respectively) and MinKNOW 2.1 v18.06.2.

Illumina sequencing library preparations

The same DNA samples were used to prepare paired-end libraries with insert size of ~680 bp, following the manufacturer's instructions for the kit NEBNext® Ultra™ II DNA (New England Biolabs Inc., Ipswich, MA, USA). The libraries were sequenced using an Illumina NextSeq500 system (Illumina NextSeq 500, [RRID:SCR.014983](#)) (serial No. NB501764).

Base-calling, adaptor trimming, and chimeric read detection

For a first assembly, reads were base-called at the European Molecular Biology Laboratory using Guppy v1.5.1 (ONT). For subsequent polishing, we used Guppy v3.0.3 (with parameters `-c dna_r9.4.1.450bps_hac.cfg`), then adaptors were trimmed with Porechop v0.2.4 (Porechop, [RRID:SCR.016967](#)) [30] with default parameters. YACRD v0.5.1 [31] with the subcommand `chimeric` and the option `-filter` was used to remove chimeric reads.

Whole-genome alignments

Genomes were aligned using LAST v979 (LAST, [RRID:SCR.006119](#)) [32]. A database was first generated (`last-db -cR01`), and then `lastal` and `last-dotplot` with default parameters were used to generate, respectively, an alignment file and a dot-plot. For the circular visualization of genome alignments, we used the command `lastal` with `-f BlastTab` parameter, then parsed the alignment to filter out short alignments and generate the links file needed by Circos (Circos, [RRID:SCR.011798](#)) [33].

Mapping of long reads

Validation of genomes during and after assembly involved rounds of read mapping. Reads were aligned with Minimap2 v2.16r922 [34] (with parameters `-ax map-ont`). The resulting mapping file was processed with Samtools v1.9 (Samtools, [RRID:SCR.002105](#)) [35] to obtain a sorted BAM file (`samtools view -bS -q 1 -F 4; samtools sort; samtools index`). Mapping results

were visualized with IGV v2.5.0 (Integrative Genomics Viewer, [RRID:SCR.011793](#)) [36].

Genome assembly

Assemblies were performed with Canu v1.7 (Canu, [RRID:SCR.015880](#)) [37] and the parameters `useGrid = False`, `genomeSize = 30m`, `correctedErrorRate = 0.16` with reads base-called by Guppy v1.5.1.

For the manual curation of the assemblies, we generated whole assembly alignments and dot-plots of Swe1, Swe2, and Swe3 two by two. For Swe1 and Swe3, Canu contigs were ordered by synthesizing the results from the 3 possible all-against-all alignments. To confirm a link between 2 contigs, we used the following strategy: when a contig of the Swe1 assembly spanned 2 contigs of Swe3, long reads of Swe1 present in this spanning area were extracted from the Swe1 corrected and trimmed reads provided by Canu. Then this set of reads was mapped on Swe2 and Swe3 assemblies. The 2 targeted contigs of Swe3 were considered “linked” if different parts of several unique reads mapped on the 2 Swe3 contigs’ ends. If the reads that supported the link had different mapping orientation (forward or reverse), 1 contig was complemented before the last step (see Solving links between contigs) to ensure a correct orientation of the final chromosome.

To guide correct assembly, we also searched for centromeres in the contigs. They were identified as highly duplicated regions in the all-against-all alignment dot-plots produced by LAST. The identification of the repeated canonical telomeric sequence (TTAGGG)_n [9] and its reverse complement (CCCTAA)_n at the beginning or end of certain contigs allowed the identification of chromosome ends. The Dan1 assembly was manually curated using a similar strategy with the Dan2 genome as a reference.

Solving links between contigs

Overlaps between linked contigs were identified by a BLASTN (NCBI BLAST, [RRID:SCR.004870](#)) [38] alignment of their last 100 kb. Any duplicate sequence was trimmed out from 1 contig and both contigs were joined. The inferred junction was then validated by verification of the underlying read support. For the linked contigs that did not overlap, the sequence in the gap was extrapolated from the reads that matched and extended the ends of contigs, on the basis of alignments at the last 1 kb of each contig. These sequences were aligned with MAFFT v7.427 (MAFFT, [RRID:SCR.011811](#)) [39]. The alignment was visualized with SeaView (SeaView, [RRID:SCR.015059](#)) [40], and only the portion of the alignment strictly between the 2 contigs sequences was kept. SeaView also generated a consensus sequence (on the basis of 60% sequence identify by default). The resulting sequence was inserted between the 2 contigs to link them and the supposed continuity verified by a further cycle of read mapping.

Assembly polishing with long reads

Genome polishing was carried out with 2 or 4 iterative runs of Racon v1.4.2 (Racon, [RRID:SCR.017642](#)) [41] and parameters `-m 8 -x -6 -g -8 -w 500`, and a run of Medaka v0.8.1 (ONT) with the parameter `-m r941.min.high`.

Mitochondrial genome circularization

Canu assembles small circular elements as contigs with tandem duplications of the element. We resolved the mitochondrial

genomes as recommended by Canu’s authors [7]. MUMmer suite v4.0.0.beta2 (MUMmer, [RRID:SCR.018171](#)) [42] was used to align the contig identified as the putative mitochondria on itself with NUCmer and parameters `-maxmatch -nosimplify`. Coordinates of a full copy were identified with the `show-coords` command and `-lrcT` parameters.

PCR

PCR was carried out to test a genome rearrangement between Swe2 and Dan2 genomes, with primers P1F (GAGATATC-GAACGTCGCATGG), P1R (ACATCAAGCCTTTGTGCGAGGA), and P3F (GCTCAGGACCGACGTACAAG). PCR reactions were run according to the GoTaq® G2 Flexi DNA polymerase instructions (Promega, Madison, WI, USA), with 50 ng of template DNA and 1 mM of each forward and reverse primer, in a final volume of 25 µL. The reaction started by initial denaturation at 95°C for 2 min, followed by 30 amplification cycles (95°C for 30 sec, 60°C for 30 sec, and 72°C for 30 sec), and a final elongation for 5 min at 72°C.

Defining a set of 305 identical proteins

Identical proteins shared by the 2 *D. coniospora* genomes available (Swe2 and Dan2) were recovered using a reciprocal best BLAST [38] hit strategy on the 2 proteomes. Proteins that were duplicated in 1 or both genomes were filtered out. The set was further refined by only retaining proteins corresponding to mono-exonic genes.

Assessment of gene sequence in ONT-only assemblies

TBLASTN searches were run using the amino acid sequence of the set of 305 identical proteins against the different nanopore-only assemblies. A gene was considered correct if the query coverage, i.e., the ratio of alignment length to the query length, was equal to 1.

Short-read polishing

Short reads were trimmed using Trimmomatic v0.39 (Trimmomatic, [RRID:SCR.011848](#)) [43] with the parameters `LEADING:3 TRAILING:3 SLIDINGWINDOW:4:30 MINLEN:36`. Then, only paired reads were mapped on assemblies with bwa v0.7.17 (BWA, [RRID:SCR.010910](#)) [44] and default parameters (`bwa index`, then `bwa mem`). The resulting mapping file was converted in BAM, sorted, and indexed with samtools. This latter file was used to polish the assembly with Pilon v1.23 (Pilon, [RRID:SCR.014731](#)) [45] with the parameters `-fix bases -vcf -mindepth 10 -minmq 20 -minqual 15 -changes -diploid`. Several iterations were conducted for each strain, until the number of changes was <5.

Flye assembly

An additional *de novo* assembly was performed with Flye v2.4.2 (Flye, [RRID:SCR.017016](#)) [8], and the parameter `-genome-size 32m`, using the ONT reads recalled by Guppy v3.0.3.

Assessing the genome integrity

The genome integrity was assessed with BUSCO v3.1.0 (BUSCO, [RRID:SCR.015008](#)) and the curated set `ascomycota_odb9` version 2016-02-13 [25]. A BLASTP search enabled Swe2 monoexonic genes present among USCOs to be identified. This list of 219

Swe2 genes was then used as a TBLASTN query against the different assemblies of Swe1 and Swe3. A gene was considered correct when it matched the corresponding Swe2 gene perfectly in length. An analogous analysis was carried out for Dan1, on the basis of the 273 Dan2 monoexonic genes that are USCOs.

Characterization of chimeric reads

Swe1 reads identified as chimeric by YACRD were aligned on the final (short-read polished) Swe1 assembly. The main alignment was identified using samtools view -F 2308. The CIGAR string was then parsed to determine whether the longest residual part of the read was 5' or 3' to the main alignment, thereby giving an orientation to the putative chimeric read and localizing the potential chimeric break point. The 500 bp of sequence 5' and 3' of this point were extracted and individually mapped back on the Swe1 final assembly and the number of unique reads in a 10-kb non-overlapping sliding window was calculated. For the reads for which both 500 bp fragments mapped on the same chromosome, the smallest distance between the 2 fragments was calculated.

Availability of Supporting Data and Materials

Genomes of the strains Swe1, Swe3, and Dan1 are available on our institute website [46]. All supporting data can be accessed at the GigaScience GigaDB database [47]. The reads used in this work can be found at the European Nucleotide Archive (ENA) under the study numbers PRJEB35969, PRJEB35970, and PRJEB35971. The raw signal runs are available under the accessions ERR3774158, ERR3774162, and ERR3774163; the FASTQ files of base-called reads (Guppy v3.0.3) are available under the accessions ERR3997391, ERR3997394, and ERR3997483; the FASTQ files of Illumina paired-end reads are available under the accessions ERR3997389, ERR3997392, and ERR3997395. Accession numbers are given in the order Swe1, Swe3, and Dan1.

Additional Files

Supplementary Figure S1. Read distribution
 Supplementary Figure S2. Swe1 assembly error
 Supplementary Figure S3. Swe3 assembly error
 Supplementary Figure S4. Canu read distribution
 Supplementary Figure S5. Chimeric read distribution
 Supplementary Figure S6. Chimeric read mapping
 Supplementary Figure S7. Dan1 and Dan2 rearrangements
 Supplementary Figure S8. Neighbourhood of Swe3 polishing errors
 Supplementary Table 1. Read coverage of the genomes. This table also contains the results for the TBLASTN on the 305 candidate identical proteins.
 Supplementary Table 2. Read support, in Swe1, Swe3, and Dan1 assemblies, for the predicted correct sequence for each homopolymer stretch in the genes corresponding to 10 of the 305 candidate identical proteins.
 Supplementary Methods. Additional methodological details.

Abbreviations

ATCC: American Type Culture Collection; BLAST: Basic Local Alignment Search Tool; bp: base pairs; BUSCO: Benchmarking Universal Single-Copy Orthologs; BWA: Burrows-Wheeler Aligner; EDTA: ethylenediaminetetraacetic acid; kb: kilobase pairs; MAFFT: Multiple Alignment using Fast Fourier Transform;

Mb: megabase pairs; NCBI: National Center for Biotechnology Information; NGMY: nematode growth medium plus yeast extract; numt: nuclear copies of mitochondrial DNA; ONT: Oxford Nanopore Technology; USCO: universal single-copy orthologue; VeCTR: very long stretches of complex tandem repeats.

Competing Interests

The authors declare that they have no competing interests.

Funding

This work was supported by institutional grants from the Institut National de la Santé et de la Recherche Médicale, Centre National de la Recherche Scientifique and Aix-Marseille University to the CIML, and the Agence Nationale de la Recherche program grant (ANR-16-CE15-0001-01), and “Investissements d’Avenir” ANR-11-LABX-0054 (Labex INFORM), ANR-16-CONV-0001, and ANR-11-IDEX-0001-02, and funding from the Excellence Initiative of Aix-Marseille University—A*MIDEX.

Authors’ Contributions

Conceptualization: J.J.E., D.C.; Methodology: D.C., J.J.E.; Investigation: J.R., J.P., D.C.; Validation: D.C.; Formal Analysis: D.C., J.P.; Resources: V.B., J.J.E.; Data Curation: J.P., D.C.; Writing—Original Draft: D.C., J.J.E.; Writing—Review & Editing: D.C., J.J.E., G.B.; Visualization: D.C.; Supervision: J.J.E., V.B., G.B.; Project Administration: J.J.E.; Funding Acquisition: J.J.E., V.B.

Acknowledgements

The authors thank Yuquan Xu and Liwen Zhang for providing access to the raw sequencing data for Dan2, Xing Zhang for help in preparing DNA samples, Lionel Spinelli for informatic support, and Nathalie Pujol and Laurent Tichit for comments.

References

1. Jansson HB, Jeyaprakash A, Zuckerman BM. Differential adhesion and infection of nematodes by the endoparasitic fungus *Meria coniospora* (Deuteromycetes). *Appl Environ Microbiol* 1985;49:552–5.
2. Pujol N, Link EM, Liu LX, et al. A reverse genetic analysis of components of the Toll signalling pathway in *Caenorhabditis elegans*. *Curr Biol* 2001;11:809–21.
3. Dierking K, Polanowska J, Omi S, et al. Unusual regulation of a STAT protein by an SLC6 family transporter in *C. elegans* epidermal innate immunity. *Cell Host Microbe* 2011;9:425–35.
4. Labeled SA, Omi S, Gut M, et al. The pseudokinase NIPI-4 is a novel regulator of antimicrobial peptide gene expression. *PLoS One* 2012;7:e33887.
5. Lebrigand K, He LD, Thakur N, et al. Comparative genomic analysis of *Drechmeria coniospora* reveals core and specific genetic requirements for fungal endoparasitism of nematodes. *PLoS Genet* 2016;12:e1006017.
6. Zhang L, Zhou Z, Guo Q, et al. Insights into adaptations to a near-obligate nematode endoparasitic lifestyle from the finished genome of *Drechmeria coniospora*. *Sci Rep* 2016;6:23122.
7. Canu 1.8 documentation. <https://canu.readthedocs.io/en/latest/faq.html#my-circular-element-is-duplicated-has-overlap>. Accessed 15 November 2019.

8. Kolmogorov M. Fast and accurate de novo assembler for single molecule sequencing reads: fenderglass/Flye. <https://github.com/fenderglass/Flye>. Accessed 3 June 2019.
9. Schechtman MG. Characterization of telomere DNA from *Neurospora crassa*. *Gene* 1990;**88**:159–65.
10. Hazkani-Covo E, Zeller RM, Martin W. Molecular poltergeists: Mitochondrial DNA copies (numts) in sequenced nuclear genomes. *PLoS Genet* 2010;**6**:e1000834.
11. Argueso JL, Westmoreland J, Mieczkowski PA, et al. Double-strand breaks associated with repetitive DNA can reshape the genome. *Proc Natl Acad Sci U S A* 2008;**105**:11845–50.
12. Sun S, Yadav V, Billmyre RB, et al. Fungal genome and mating system transitions facilitated by chromosomal translocations involving intercentromeric recombination. *PLoS Biol* 2017;**15**:e2002527.
13. TransposonPSI: An Application of PSI-Blast to Mine (Retro-)Transposon ORF Homologies. <http://transposonpsi.sourceforge.net>. Accessed 1 April 2020.
14. Hubley R, Finn RD, Clements J, et al. The Dfam database of repetitive DNA families. *Nucleic Acids Res* 2016;**44**:D81–9.
15. Senol Cali D, Kim JS, Ghose S, et al. Nanopore sequencing technology and tools for genome assembly: Computational analysis of the current state, bottlenecks and future directions. *Brief Bioinform* 2019;**20**:1542–59.
16. Scheunert A, Dorfner M, Lingl T, et al. Can we use it? On the utility of de novo and reference-based assembly of Nanopore data for plant plastome sequencing. *PLoS One* 2020;**15**:e0226234.
17. White R, Pellefigues C, Ronchese F, et al. Investigation of chimeric reads using the MinION. *F1000Res* 2017;**6**:631.
18. Eccles D, Chandler J, Camberis M, et al. De novo assembly of the complex genome of *Nippostrongylus brasiliensis* using MinION long reads. *BMC Biol* 2018;**16**:6.
19. Schmid M, Frei D, Patrignani A, et al. Pushing the limits of de novo genome assembly for complex prokaryotic genomes harboring very long, near identical repeats. *Nucleic Acids Res* 2018;**46**:8953–65.
20. Watson M, Warr A. Errors in long-read assemblies can critically affect protein prediction. *Nat Biotechnol* 2019;**37**:124–6.
21. Wick RR, Judd LM, Holt KE. Performance of neural network basecalling tools for Oxford Nanopore sequencing. *Genome Biol* 2019;**20**:129.
22. Somerville V, Lutz S, Schmid M, et al. Long-read based de novo assembly of low-complexity metagenome samples results in finished genomes and reveals insights into strain diversity and an active phage system. *BMC Microbiol* 2019;**19**:143.
23. Dal Molin A, Minio A, Griggio F, et al. The genome assembly of the fungal pathogen *Pyrenochaeta lycopersici* from Single-Molecule Real-Time sequencing sheds new light on its biological complexity. *PLoS One* 2018;**13**:e0200217.
24. Jain M, Koren S, Miga KH, et al. Nanopore sequencing and assembly of a human genome with ultra-long reads. *Nat Biotechnol* 2018;**36**:338–45.
25. Simao FA, Waterhouse RM, Ioannidis P, et al. BUSCO: Assessing genome assembly and annotation completeness with single-copy orthologs. *Bioinformatics* 2015;**31**:3210–2.
26. He LD, Ewbank JJ. Polyethylene glycol-mediated transformation of *Drechmeria coniospora*. *Bio Protoc* 2017;**7**:e2157.
27. Fungal DNA extraction protocol. <https://www.pnas.org/content/pnas/suppl/2018/01/08/1715954115.DCSupplemental/pnas.1715954115.sapp.pdf>. Accessed 16 April 2020.
28. Kjærboelling I, Vesth TC, Frisvad JC, et al. Linking secondary metabolites to gene clusters through genome sequencing of six diverse *Aspergillus* species. *Proc Natl Acad Sci U S A* 2018;**115**:E753–61.
29. Quick J. Ultra-long read sequencing protocol for RAD004 v3. protocols.io 2018 <https://dx.doi.org/10.17504/protocols.io.mrxc57n>
30. Wick R. Porechop. <https://github.com/rwick/Porechop>. Accessed 3 December 2019.
31. Marijon P, Chikhi R, Varré J-S. yacr and fpa: Upstream tools for long-read genome assembly. *Bioinformatics* 2020;**36**:3894–6.
32. Kielbasa SM, Wan R, Sato K, et al. Adaptive seeds tame genomic sequence comparison. *Genome Res* 2011;**21**:487–93.
33. Krzywinski M, Schein J, Birol I, et al. Circos: An information aesthetic for comparative genomics. *Genome Res* 2009;**19**:1639–45.
34. Li H. Minimap2: Pairwise alignment for nucleotide sequences. *Bioinformatics* 2018;**34**:3094–100.
35. Li H, Handsaker B, Wysoker A, et al. The Sequence Alignment/Map format and SAMtools. *Bioinformatics* 2009;**25**:2078–9.
36. Thorvaldsdóttir H, Robinson JT, Mesirov JP. Integrative Genomics Viewer (IGV): High-performance genomics data visualization and exploration. *Brief Bioinform* 2013;**14**:178–92.
37. Koren S, Walenz BP, Berlin K, et al. Canu: Scalable and accurate long-read assembly via adaptive k-mer weighting and repeat separation. *Genome Res* 2017;**27**:722–36.
38. Altschul SF, Gish W, Miller W, et al. Basic Local Alignment Search Tool. *J Mol Biol* 1990;**215**:403–10.
39. Katoh K, Standley DM. MAFFT multiple sequence alignment software version 7: Improvements in performance and usability. *Mol Biol Evol* 2013;**30**:772–80.
40. Gouy M, Guindon S, Gascuel O. SeaView Version 4: A multiplatform graphical user interface for sequence alignment and phylogenetic tree building. *Mol Biol Evol* 2010;**27**:221–4.
41. Vaser R, Sović I, Nagarajan N, et al. Fast and accurate de novo genome assembly from long uncorrected reads. *Genome Res* 2017;**27**:737–46.
42. Kurtz S, Phillippy A, Delcher AL, et al. Versatile and open software for comparing large genomes. *Genome Biol* 2004;**5**:R12.
43. Bolger AM, Lohse M, Usadel B. Trimmomatic: A flexible trimmer for Illumina sequence data. *Bioinformatics* 2014;**30**:2114–20.
44. Li H. Aligning sequence reads, clone sequences and assembly contigs with BWA-MEM. ArXiv 2013:1303.3997.
45. Walker BJ, Abeel T, Shea T, et al. Pilon: An integrated tool for comprehensive microbial variant detection and genome assembly improvement. *PLoS One* 2014;**9**:e112963.
46. The CIML website. <http://www.ciml.univ-mrs.fr/application/DC/Genome.htm>. Accessed 31 August 2020.
47. Courtine D, Provaznik J, Reboul J, et al. Supporting data for “Long-read only assembly of *Drechmeria coniospora* genomes reveals widespread chromosome plasticity and illustrates the limitations of current nanopore methods.” GigaScience Database 2020. <http://dx.doi.org/10.5524/100776>.